ACS APPLIED MATERIALS & INTERFACES

Research Article

www.acsami.org

Fabrication of $Cu_2ZnSn(S,Se)_4$ Solar Cells via an Ethanol-Based Sol–Gel Route Using SnS_2 as Sn Source

Wangen Zhao, Gang Wang, Qingwen Tian, Yanchun Yang, Lijian Huang, and Daocheng Pan*

State Key Laboratory of Rare Earth Resource Utilization, Changchun Institute of Applied Chemistry, Chinese Academy of Sciences, 5625 Renmin Street, Changchun, Jilin 130022, China

Supporting Information

ABSTRACT: $Cu_2ZnSn(S,Se)_4$ semiconductor is a promising absorber layer material in thin film solar cells due to its own virtues. In this work, high quality $Cu_2ZnSn(S,Se)_4$ thin films have been successfully fabricated by an ethanol-based sol–gel approach. Different from those conventional sol–gel approaches, SnS_2 was used as the tin source to replace the most commonly used $SnCl_2$ in order to avoid the possible chlorine contamination. In addition, sodium was found to improve the short-circuit current and fill factor rather than the open-circuit voltage due to the decrease of the thickness of small-grained layer. The selenized $Cu_2ZnSn(S,Se)_4$ thin films showed large densely packed grains and smooth surface morphology, and a power conversion efficiency of 6.52% has been realized for $Cu_2ZnSn(S,Se)_4$ thin film solar cell without antireflective coating.

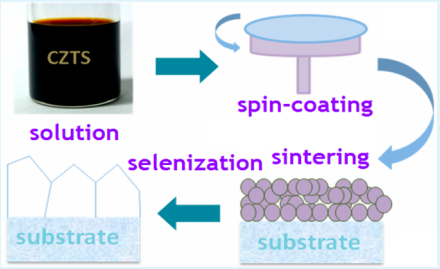

KEYWORDS: *CZTSSe, thin film solar cells, kesterite, SnS_2, solution process*

INTRODUCTION

Kesterite-type $Cu_2ZnSn(S,Se)_4$ (CZTSSe) semiconductor is considered as one of the most prospective photovoltaic materials, which has taken the limelight over the past two decades because of its low toxicity, high abundance, and low material cost for larger possibility of commercial production compared to another important Cu-based $Cu(In,Ga)(S,Se)_2$ (CIGSSe) semiconductor with a record power conversion efficiency (PCE) of 20.4%.[1] To minimize the manufacturing cost of CZTSSe thin film solar cells, various nonvacuum-based deposition approaches have been reported, including electrodeposition approach,[2−4] milling dispersion approach,[5] nanoparticle-based approach,[6−10] hydrazine-based approach,[11−13] sol–gel approach,[14−18] etc. Among these solution-based methods, the latter three approaches have made greater progresses. Recently, a record power conversion efficiency of 10.2% and 12.6% have been achieved for CZTSSe thin film solar cells by a nanoparticle-based approach and a hydrazine-based solution approach, respectively.[19,20] Because of the complex synthesis of CZTS nanoparticles and high toxicity of hydrazine, the sol–gel approach based on rather simple and safe preparation process has drawn a great deal of attention[14−18] since Hillhouse and co-workers developed a low-cost and low-toxicity sol–gel approach to fabricate CZTSSe solar cells with a power conversion efficiency of 4.1% in 2011.[14] The CZTS sol–gel solution was prepared by dissolving copper acetate, zinc chloride, tin(II) chloride, and thiourea in dimethyl sulfoxide (DMSO). Recently, the power conversion efficiency has been further enhanced to 8.3% by changing the preparation procedure of CZTS precursor solution.[15] Since 2011, some research groups modified this solution approach by using low-toxicity 2-methoxyethanol[16] or the mixture of ethanol and water[17] to replace DMSO. However, in this approach and its variants, tin(II) chloride was always used as the tin source, which may result in chlorine contamination.[16]

In this work, we presented a facile and low-toxic solution route by dissolving copper acetate, zinc acetate, and tin disulfide in butylamine/sulfur solution, and nontoxic ethanol was used as the solvent. Here, copper acetate and zinc acetate were chosen as the Cu and Zn sources. Importantly, tin(IV) disulfide was used to substitute the commonly used tin(II) chloride, which is first employed to avoid the impact of chlorine on the performance of CZTSSe solar cells except for hydrazine-based approach.[13] Meanwhile, highly reactive S powder was employed as the sulfur source to replace low reactive thiourea.

EXPERIMENTAL SECTION

Materials. Copper(II) acetate monohydrate ($Cu(Ac)_2·H_2O$, 99%), zinc acetate ($Zn(Ac)_2$, 99.99%), tin(IV) chloride ($SnCl_4$, 99%), ammonium sulfide solution ($(NH_4)_2S$, 40–48 wt %), 1-butylamine ($CH_3(CH_2)_3NH_2$, 99%), 3-mercaptopropionic acid ($HSCH_2CH_2COOH$, 98%), cadmium sulfate ($CdSO_4$, ACS), sodium diethyldithiocarbamate trihydrate ($NaS_2N(CH_3)_2·3H_2O$ ACS), thiourea ($(NH_2)_2CS$, ACS), ammonia solution ($NH_3·H_2O$, 25%), and ethanol (AR) were purchased from Aladdin. All chemicals and solvents were used as received without any further purification.

Synthesis of SnS_2. Ten and a half grams (~30 mmol) of $SnCl_4$ was dissolved in 90 mL of deionized water under magnetic stirring. Then, 9.3 mL (~60 mmol) of ammonium sulfide solution was added dropwise to the above solution, resulting in the formation of yellow

Received: April 30, 2014
Accepted: July 7, 2014
Published: July 7, 2014

precipitation. After the centrifugation and repeated washing, the yellow precipitate was attained and dried in an oven at the temperature of 80 °C. Finally, the yellow precipitate was ground into fine powder.

Preparation of the CZTS Precursor Solutions. First, 2.0 mmol of S powder was dissolved in 2.0 mL (~20 mmol) of 1-butylamine in a glass vial under magnetic stirring at room temperature. Next, 1.0 mmol of SnS_2 powder was loaded into the butylamine/S solution with continued stirring until a black brown solution was formed. Subsequently, 0.6 mL (~6 mmol) of 3-mercaptopropionic acid was added into above solution, forming a light yellow solution. Then, 1.2 mmol of zinc acetate, 1.65 mmol of copper acetate, and 5.0 mL of ethanol were putted into the above solution, forming a homogeneous and light black CZTS precursor solution after stirring for ~30 min. Finally, the CZTS precursor solution was centrifuged at 12 000 rpm for 5 min. These preparation procedures were conducted in air.

Deposition of CZTS Thin Films and Fabrication of CZTSSe Solar Cell Devices. CZTS thin films were spun on a Mo-coated glass slide (20 × 20 × 0.5 mm) at 3 000 rpm for 20 s, followed by a sintering process on a ceramic hot plate at 320 °C for 2 min. CZTS nanocrystal thin film with a thickness of ~1.5 μm was built up by repeating seven spin-coating/sintering cycles. Subsequently, the as-prepared CZTS thin films were annealed under Se vapor. Two pieces of CZTS thin films were selenized in a graphite box in the presence of approximately 0.4 g of Se pellets in a rapid temperature processing (RTP) furnace at different temperatures of 500 °C/530 °C/560 °C for 8 or 15 min in order to optimize selenization conditions. The CZTSSe solar cell devices were completed by the successive deposition of CdS thin film (~60 nm), *i*-ZnO (~70 nm), and ITO (~300 nm). Finally, metallic Al grid electrode (~1 μm) was thermally evaporated on the top of the solar cell. No antireflection layer was applied. The four cells on one substrate were separated by mechanical scribing using a tungsten needle. The active area of a device is 0.368 cm^2, excluding the area of Al grid electrode (~10%) in the total area.

Characterizations. The thermal stability of CZTS precursor was investigated by thermogravimetric analysis (TGA) on a TGA/DSC 1 STARe of Mettler-Toledo. A step profiler (AMBIOS, XP-100) was employed to measure the thickness of the thin film. The XRD patterns were recorded using a Bruker D8 X-ray diffractometer with a Cu Kα radiation source (λ = 0.15405 nm). The top-view and cross-sectional SEM images were taken on a Hitachi S-4800, and chemical composition was determined by energy dispersive X-ray (EDX) analyzer (Bruker AXS XFlash detector 4010) attached to Hitachi S-4800. Raman spectrum was tested by Renishaw RM1000 with 532 nm laser excitation. *J*–*V* curves were measured with a Keithley 2400 source meter and a solar simulator (Abet Sun 2000, AM 1.5, 100 mW/cm^2). The external quantum efficiency (EQE) measurement was conducted by a Zolix SCS100 QE system equipped with a 150 W xenon light source and a lock-in amplifier.

RESULTS AND DISCUSSION

It has been reported that SnS_2 can be dissolved in the solution of $(NH_4)_2S$ and $(N_2H_5)_2S$, forming soluble $Sn_2S_6^{2-}$ ions.[21,22] Polysulfide S_x^{2-} (x = 1–7) ions play a key role in the dissolution of SnS_2.[23] According to some reports in literature, S_x^{2-} ions were formed by the reaction of elemental sulfur with organic amines.[24] Thus, it is quite possible that SnS_2 can be dissolved in organic amine/sulfur solution. To confirm this hypothesis, SnS_2 powder was added to the butylamine/sulfur solution and a homogeneous and black brown solution was attained. Then, a small amount of 3-mercaptopropionic acid (MPA) was added to prevent precipitate formation upon the addition of Cu^{2+} and Zn^{2+} ions because MPA has a strong binding ability with Cu^{2+} and Zn^{2+} ions. As can been seen in Figure 1 (left), a light yellow solution was formed after addition of MPA, which may be attributed to the reaction of carboxyl and amino groups. Afterward, $Cu(Ac)_2{\cdot}H_2O$ and $Zn(Ac)_2$ are loaded into the above solution. Finally, nontoxic ethanol was used as the solvent to dilute the concentration and adjust the viscosity of CZTS precursor solution. The acquired light black CZTS precursor solution is shown in Figure 1 (right), which is stable in air. CZTS nanocrystal thin films were obtained by a spin-coating process, followed by a sintering process at 320 °C according to TGA result of CZTS precursor (see Figure 2a).

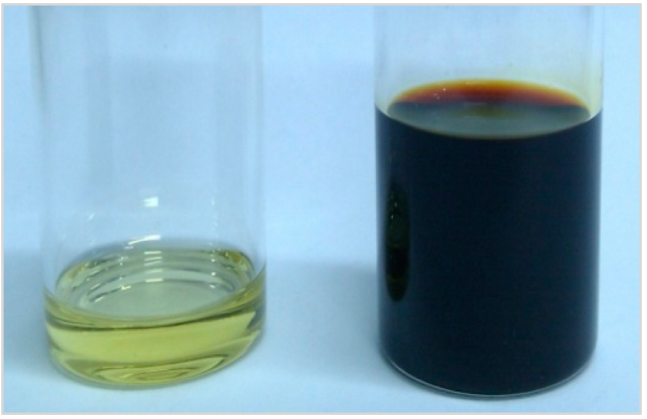

Figure 1. Photographs of SnS_2 solution (left) and CZTS precursor solution (right).

The plain-view and cross-sectional SEM images of as-prepared CZTS nanocrystal thin films on Mo-based soda-lime glass were shown in Figure S1 in the Supporting Information. It should be noted that the as-prepared CZTS thin films exhibited some obvious cracks. In order to eliminate cracks and induce nanocrystal growth, CZTS thin films were selenized at high temperatures under selenium vapor in a graphite box with a 1 mm hole on the top of the lid, as exhibited in Figure S2 in the Supporting Information. At first, the CZTSSe thin films selenized at 530 °C for 8 and 15 min were analyzed by X-ray diffraction (XRD), as shown in Figure 2b. It was obvious that the XRD peaks of CZTSSe thin films selenized for 15 min significantly became stronger and sharper; the inset of Figure 2b shows a comparison of the enlarged (112) planes of the CZTSSe thin films selenization for 8 and 15 min, indicating the increase of the crystallinity and the grain size of CZTSSe thin film with prolonged selenization time. XRD analysis of the selenized CZTSSe thin films revealed a typical kesterite structure, and binary or ternary impurity phases such as ZnSe, $SnSe_2$, and Cu_2SnSe_3 were not observed. However, the presence of ZnSe, $SnSe_2$, and Cu_2SnSe_3 impurities cannot be ruled out since their XRD patterns are very close to that of CZTSSe.[25] A pure kesterite structure is crucial to the performance of kesterite solar cells. To further confirm the crystal structure of CZTSSe thin films in the absence of secondary phases (e.g., ZnSe, $SnSe_2$, and Cu_2SnSe_3 etc.), Raman spectra were measured. As demonstrated in Figure 2c, four prominent peaks located at 173, 196, 237, and 328 cm^{-1}, which are in good agreement with those of previously reported kesterite CZTSSe thin films.[18] The complementary studies based on XRD and Raman spectroscopy confirmed that the pure phase CZTSSe thin films were achieved after the selenization at 530 °C for 8 and 15 min.

To obtain high-performance CZTSSe solar cells, we need to optimize not only the purity of the crystal phase but also the Cu-poor and Zn-rich composition of CZTSSe thin film. Cu-poor composition is beneficial for the formation of Cu vacancies, which gives rise to shallow acceptors in the CZTSSe thin film, whereas Zn-rich composition is used to avoid the formation of the substitution of Cu at Zn sites, which results in

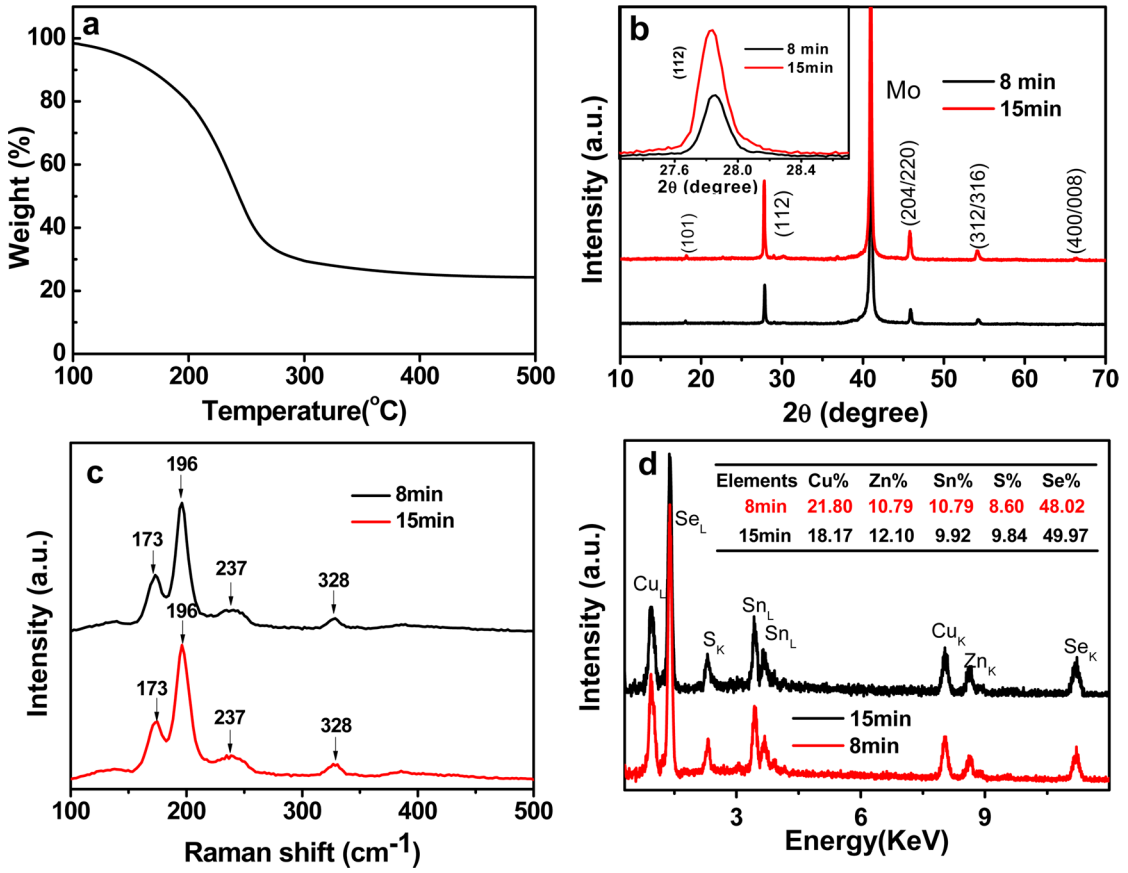

Figure 2. (a) TGA curve of CZTS precursor measured from 100 to 500 °C under N_2 atmosphere at a rate of 10 °C/min. (b) XRD pattern (inset: the comparison of (112) planes), (c) Raman spectra, and (d) chemical compositions of CZTSSe thin films selenized at the temperature of 530 °C for 8 and 15 min.

relatively deep acceptors.[26] The selenized CZTSSe thin film at 530 °C for 8 min consisted of approximately 21.8% Cu, 10.8% Zn, 10.8% Sn, 8.6% S, and 48.0% Se. Thereby, a near stoichiometric $Cu_{2.0}Zn_{1.0}Sn_{1.0}S_{0.8}Se_{4.4}$ thin film with a Cu/(Zn +Sn) ratio of 1.0 and Zn/Sn ratio of 1.0 was formed. When the selenization time was 15 min, highly desirable composition of $Cu_{1.83}Zn_{1.22}Sn_{1.0}S_{0.99}Se_{5.03}$ was obtained (see Figure 2d). It can be explained by the phase formation mechanism of CZTSSe,[27] and Cu_2S phase appeared on the surface of thin films at the early stage of selenization and single phase CZTSSe thin films were formed with prolonged selenization time.

Except for the crystal structure and chemical composition, the surface morphology of the CZTSSe thin films is one of the most important factors that affect the performance of CZTSSe devices. Densely packed and large grained Cu-based thin films are always highly desirable. It is well-known that the selenization time is directly related to the crystal growth of CZTSSe thin film. Images a and b in Figure 3 show the top-view SEM images of selenized CZTSSe thin films at 530 °C for 8 and 15 min, respectively. The grain sizes slightly increase when the selenization time was changed from 8 to 15 min. Larger grain will reduce the chance of electron and hole recombination because there is less grain boundary. Thus, prolonged selenization time has a beneficial effect on the grain growth and device performance. However, with further increase of the selenization time, Sn loss and phase separation will occur, which are detrimental to the photoelectric conversion efficiency of CZTSSe devices. Meanwhile, it was noted that the thickness

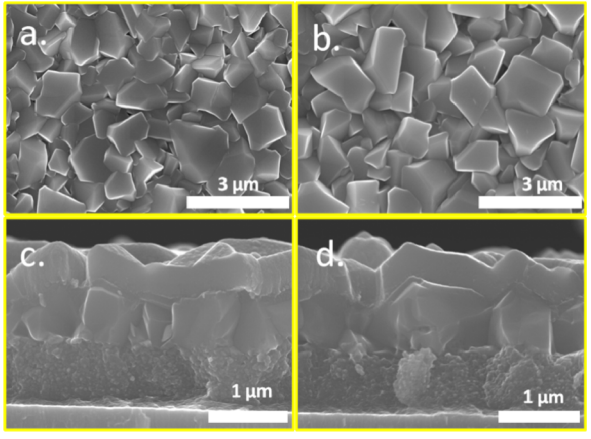

Figure 3. Top-view SEM images of selenized CZTSSe thin films at the temperature of 530 °C for (a) 8 min and (b) 15 min; (c, d) cross-sectional SEM images of the corresponding CZTSSe solar cell devices.

of the small-grained layer did not clearly decrease with prolonged selenization time, as seen in Figure 3c, d.

In addition, the effect of the different selenization temperatures on the crystal quality and morphology of CZTSSe thin films were also studied while keeping the same selenization time (15 min). At the different selenization temperatures of 500, 530, and 560 °C, their plain-view SEM images of CZTSSe thin films and the cross-sectional SEM images of corresponding CZTSSe devices are shown in Figure S3 in the Supporting

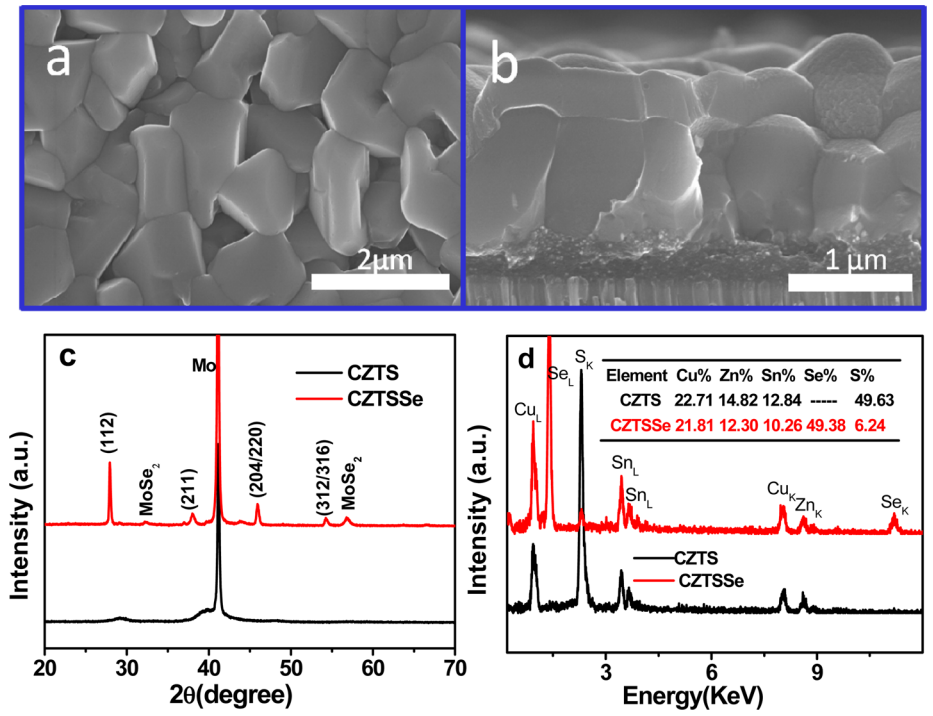

Figure 4. (a) Surface SEM image of Na-doped CZTSSe thin film; (b) cross-section SEM image of Na-doped CZTSSe device; (c) XRD patterns, (d) EDS spectra and chemical compositions of as-prepared CZTS (black) and selenized CZTSSe (red) thin films.

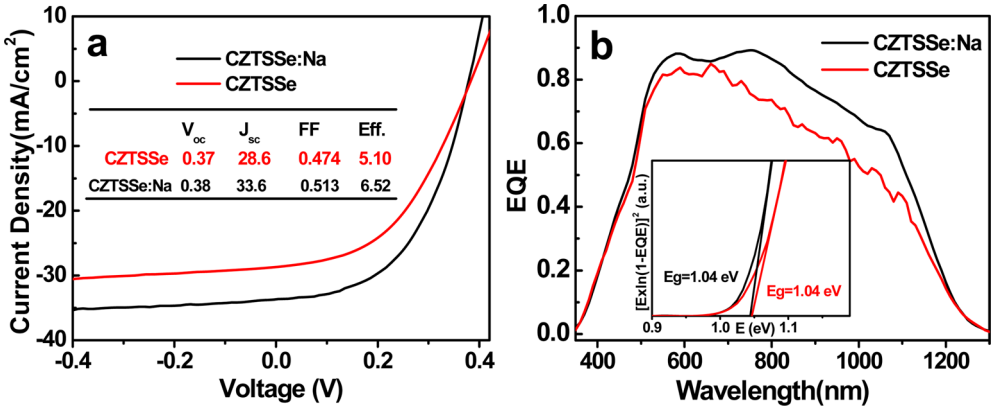

Figure 5. (a) $J-V$ curves and the performance parameters of CZTSSe and Na-doped CZTSSe solar cells under simulated solar light (AM 1.5 G) illumination. (b) External quantum efficiency (EQE) spectra of CZTSSe and Na-doped CZTSSe solar cells; inset: the corresponding band gaps were determined by plotting $[E\times\ln(1\text{-EQE})]^2$ vs E curves.

Information. With the enhancement of the selenization temperature, the selenized CZTSSe thin films exhibit higher crystallinity and a thinner small-grained bottom layer. Meanwhile, some white spots on the surface of the CZTSSe thin films were observed, indicating that the phase separation occurs. Comprehensive analysis of selenized CZTSSe thin films from SEM, XRD, and EDS, the optimal selenization condition was found to be 530 °C and 15 min.

Under the optimal selenization condition, CZTSSe thin film exhibits a bilayer structure, consisting of a large-grained top layer and a small-grained bottom layer. A thick small-grained bottom layer will increase the series resistance of devices, which will be detrimental to the photoelectric conversion efficiency of CZTSSe solar cells. It was reported that Na can induce the crystal growth of CZTSSe thin films.[28−30] To reduce or even eliminate the small-grained bottom layer, we added 1% of sodium diethyldithiocarbamate to induce the grain growth and reduce the thickness of small-grained layer. Images a and b in Figure 4 show the surface SEM image of Na-doped CZTSSe thin film and cross-sectional SEM image of the corresponding CZTSSe solar cell device. It was observed that the addition of Na significantly changed the morphology of grain (Figure 4a), which made it seem less angular and much smoother. Moreover, the thickness of small-grained bottom layer evidently decreased (Figure 4b), which could improve the performance of the CZTSSe device to some degree (especially in current density because of the decrease in series resistance and the increase of the thickness of the absorber layer). The XRD and EDS were also conducted to characterize the Na-doped CZTSSe absorber layer, confirming that a highly crystalline CZTSSe thin film with a suitable composition was obtained. Some minor diffraction peaks appeared on Na-doped XRD pattern (Figure 4c), which were not shown on that of undoped CZTSSe thin films. Different from undoped CZTSSe thin films,

a thin $MoSe_2$ layer was observed by XRD and SEM. Our experimental results confirmed that the incorporation of Na can induce the crystal growth of CZTSSe thin film and decrease the thickness of small-grained layer.

In addition, because of the different valence states of Cu and Sn ions, X-ray photoelectron spectroscopy (XPS) was used to identify the valence states of Cu and Sn ions in CZTSSe thin film, as shown in Figure S4 in the Supporting Information. It can be seen that Cu 2p peaks located at 931.7 and 951.6 eV with a splitting value of 19.9 eV, and Sn 3d peaks located at 486.7 and 495.3 eV with a splitting value of 8.6 eV, corresponding to Cu^+ and Sn^{4+} ions, respectively.

Figure 5a shows a comparison of $J-V$ curves for CZTSSe and Na-doped CZTSSe solar cells. A significant improvement in PCE was observed from 5.10% to 6.50% for Na-doped CZTSSe solar cell. This improvement is mainly due to the increase in short circuit current density (J_{SC}) and fill factor (FF). As mentioned above, the incorporation of Na can increase the thickness of large-grained top layer, which will improve the photoresponse of CZTSSe absorber layer and thereby enhance J_{SC}. External quantum efficiency (EQE) spectra of the CZTSSe and Na-doped CZTSSe solar cells were measured and shown in Figure 5b. It was also revealed that the J_{SC} increase is due to a stronger photoresponse at the near-infrared (NIR) region instead of a lower band gap for Na-doped CZTSSe solar cells since CZTSSe and Na-doped CZTSSe thin films have the same band gap of 1.04 eV (see the inset of Figure 5b). According to the analysis of light $J-V$ curves of the CZTSSe and Na-doped CZTSSe solar cells, Na-doped CZTSSe solar cells possess a lower series resistance (R_s) (1.57 vs 3.53 Ω cm^2, see Figure S5 in the Supporting Information) because of a thinner small-grained bottom layer, which is beneficial to achieving a high *FF*.

CONCLUSIONS

In summary, we have demonstrated a simple solution-based approach for depositing high quality CZTSSe thin films, in which all the precursors were easily available and mixed at a molecular level without the need of highly toxic chemicals. SnS_2 was used to replace commonly used $SnCl_2$ as the tin source, which may eliminate the effect of chlorine impurity on the performance of CZTSSe device. In addition, sulfur powder was used as the S source to substitute low reactive thiourea. It was found that the incorporation of Na can induce the grain growth of CZTSSe thin films and decrease the thickness of the small-grained layer, which led to significant improvement in both J_{SC} and FF. A power conversion efficiency of 6.52% has been achieved for Na-doped CZTSSe solar cells, which is expected to further enhance by completely eliminating small-grained bottom layer. Moreover, this solution approach could be extended to the fabrication of other Cu-based semiconductor thin films, such as $Cu_2FeSn(S,Se)_4$, $Cu_2CoSn(S,Se)_4$, $Cu_2NiSn(S,Se)_4$, $Cu_2CdSn(S,Se)_4$, etc.

ASSOCIATED CONTENT

Supporting Information

The plain-view and cross-sectional SEM images of as-prepared CZTS nanocrystal thin film. The digital pictures of graphite box, selenized CZTSSe thin film, and a completed CZTSSe solar cell device. The top-view and cross-sectional SEM images of selenized CZTSSe thin films at temperatures of 500 °C/530 °C/560 °C for 15 min. X-ray photoelectron spectroscopy (XPS) spectra of selenized CZTSSe thin film. The analysis of light $J-V$ curves of CZTSSe and Na-doped CZTSSe solar cells. This material is available free of charge via the Internet at http://pubs.acs.org.

AUTHOR INFORMATION

Corresponding Author

*E-mail: pan@ciac.ac.cn.

Notes

The authors declare no competing financial interest.

ACKNOWLEDGMENTS

This work was supported by the National Natural Science Foundation of China (Grants 91333108, 51302258, 51172229, and 51202241).

REFERENCES

(1) Jackson, P.; Hariskos, D.; Lotter, E.; Paetel, S.; Wuerz, R.; Menner, R.; Wischmann, W.; Powalla, M. New World Record Efficiency for $Cu(In,Ga)Se_2$ Thin-Film Solar Cells Beyond 20%. *Prog. Photovoltaics* **2011**, *19*, 894−897.

(2) Guo, L.; Zhu, Y.; Gunawan, O.; Gokmen, T.; Deline, V. R.; Ahmed, S.; Romankiw, L. T.; Deligianni, H. Electrodeposited $Cu_2ZnSnSe_4$ Thin Film Solar Cell with 7% Power Conversion Efficiency. *Prog. Photovoltaics* **2014**, *22*, 58−68.

(3) Ahmed, S.; Reuter, K. B.; Gunawan, O.; Guo, L.; Romankiw, L. T.; Deligianni, H. A High Efficiency Electrodeposited Cu_2ZnSnS_4 Solar Cell. *Adv. Energy Mater.* **2012**, *2*, 253−259.

(4) Ge, J.; Jiang, J.; Yang, P.; Peng, C.; Huang, Z.; Zuo, S.; Yang, L.; Chu, J. A 5.5% Efficient Co-electrodeposited ZnO/CdS/Cu_2ZnSnS_4/Mo Thin Film Solar Cell. *Sol. Energy Mater. Sol. Cells* **2014**, *125*, 20−26.

(5) Woo, K.; Kim, Y.; Moon, J. A Non-Toxic, Solution-Processed, Earth Abundant Absorbing Layer for Thin-Film Solar Cells. *Energy Environ. Sci.* **2012**, *5*, 5340−5345.

(6) Cao, Y.; Denny, M. S., Jr.; Caspar, J. V.; Farneth, W. E.; Guo, Q.; Ionkin, A. S.; Johnson, L. K.; Lu, M.; Malajovich, I.; Radu, D.; Rosenfeld, H. D.; Choudhury, K. R.; Wu, W. High-Efficiency Solution-Processed $Cu_2ZnSn(S,Se)_4$ Thin-Film Solar Cells Prepared from Binary and Ternary Nanoparticles. *J. Am. Chem. Soc.* **2012**, *134*, 15644−15647.

(7) Guo, Q.; Ford, G. M.; Yang, W. C.; Walker, B. C.; Stach, E. A.; Hillhouse, H. W.; Agrawal, R. Fabrication of 7.2% Efficient CZTSSe Solar Cells Using CZTS Nanocrystals. *J. Am. Chem. Soc.* **2010**, *132*, 17384−17386.

(8) Zhou, H.; Hsu, W.-C.; Duan, H. S.; Bob, B.; Yang, W.; Song, T.-B.; Hsu, C.-J.; Yang, Y. CZTS Nanocrystals: A Promising Approach for Next Generation Thin Film Photovoltaics. *Energy Environ. Sci.* **2013**, *6*, 2822−2838.

(9) Wu, W.; Cao, Y.; Caspar, J. V.; Guo, Q.; Johnson, L. K.; Malajovich, I.; Rosenfeld, H. D.; Choudhury, K. R. Studies of The Fine-Grain Sub-layer in The Printed CZTSSe Photovoltaic Devices. *J. Mater. Chem. C* **2014**, *2*, 3777−3781.

(10) Miskin, C. K.; Yang, W. C.; Hages, C. J.; Carter, N. J.; Joglekar, C. S.; Stach, E. A.; Agrawal, R. 9.0% Efficient $Cu_2ZnSn(S,Se)_4$ Solar Cells From Selenized Nanoparticle Inks. *Prog. Photovoltaics* **2014**, DOI: 10.1002/pip.2472 (Accessed: 18th Feb 2014).

(11) Bag, S.; Gunawan, O.; Gokmen, T.; Zhu, Y.; Todorov, T. K.; Mitzi, D. B. Low Band Gap Liquid-Processed CZTSe Solar Cell with 10.1% Efficiency. *Energy Environ. Sci.* **2012**, *5*, 7060−7065.

(12) Todorov, T. K.; Tang, J.; Bag, S.; Gunawan, O.; Gokmen, T.; Zhu, Y.; Mitzi, D. B. Beyond 11% Efficiency: Characteristics of State-of-the-Art $Cu_2ZnSn(S,Se)_4$ Solar Cells. *Adv. Energy Mater.* **2013**, *3*, 34−38.

(13) Yang, W.; Duan, H. S.; Bob, B.; Zhou, H.; Lei, B.; Chung, C. H.; Li, S. H.; Hou, W. W.; Yang, Y. Novel Solution Processing of High-Efficiency Earth-Abundant $Cu_2ZnSn(S,Se)_4$ Solar Cells. *Adv. Mater.* **2012**, *24*, 6323−6329.

(14) Ki, W.; Hillhouse, H. W. Earth-Abundant Element Photovoltaics Directly from Soluble Precursors with High Yield Using a Non-Toxic Solvent. *Adv. Energy Mater.* **2011**, *1*, 732−735.
(15) Xin, H.; Katahara, J. K.; Braly, I. L.; Hillhouse, H. W. 8% Efficient $Cu_2ZnSn(S,Se)_4$ Solar Cells from Redox Equilibrated Simple Precursors in DMSO. *Adv. Energy Mater.* **2014**, DOI: 10.1002/aenm.201301823 (Accessed 1st Apr 2014).
(16) Su, Z.; Sun, K.; Han, Z.; Cui, H.; Liu, F.; Lai, Y.; Li, J.; Hao, X.; Liu, Y.; Green, M. A. Fabrication of Cu_2ZnSnS_4 Solar Cells with 5.1% Efficiency via Thermal Decomposition and Reaction Using a Non-Toxic Sol−Gel Route. *J. Mater. Chem. A* **2014**, *2*, 500−509.
(17) Jiang, M.; Lan, F.; Yan, X.; Li, G. $Cu_2ZnSn(S_{1-x}Se_x)_4$ Thin Film Solar Cells Prepared by Water-Based Solution Process. *Phys. Status Solidi RRL* **2014**, *8*, 223−227.
(18) Schnabel, T.; Löw, M.; Ahlswede, E. Vacuum-Free Preparation of 7.5% Efficient $Cu_2ZnSn(S,Se)_4$ Solar Cells Based on Metal Salt Precursors. *Sol. Energy Mater. Sol. Cells* **2013**, *117*, 324−328.
(19) Leidholm, C.; Hotz, C.; Breeze, A.; Sunderland C.; Ki, W. Sintered CZTS Nanoparticle Solar Cells on Metal Foil. NREL Subcontract Report NREL/SR-5200−56510, 2012(Accessed: 1st Sep 2012) .
(20) Wang, W.; Winkler, M. T.; Gunawan, O.; Gokmen, T.; Todorov, T. K.; Zhu, Y.; Mitzi, D. B. Device Characteristics of CZTSSe Thin-Film Solar Cells with 12.6% Efficiency. *Adv. Energy Mater.* **2013**, DOI: 10.1002/aenm.201301465 (Accessed 27th Nov 2013).
(21) Yeon, P. H.; Yoon, Y.; Oh, S. W.; Nam, S.; Pak, Y. N. Continuous Preconcentration of $Sn^{2+/}Sn^{4+}$ by the On-line Sulfide Precipitation-Dissolution. *Bull. Korean Chem. Soc.* **2004**, *25*, 1156−1160.
(22) Mitzi, D. B. Solution Processing of Chalcogenide Semiconductors via Dimensional Reduction. *Adv. Mater.* **2009**, *21*, 3141−3158.
(23) Kovalenko, M. V.; Bodnarchuk, M. I.; Zaumseil, J.; Lee, J.; Talapin, D. V. Expanding the Chemical Versatility of Colloidal Nanocrystals Capped with Molecular Metal Chalcogenide Ligands. *J. Am. Chem. Soc.* **2010**, *132*, 10085−10092.
(24) Sasaki, Y.; Olsen, F. P. Reactions of Benzylamine with Sulfur. *Can. J. Chem.* **1971**, *49*, 283−293.
(25) Walsh, A.; Chen, S.; Wei, S. H.; Gong, X. G. Kesterite Thin-Film Solar Cells: Advances in Materials Modelling of Cu_2ZnSnS_4. *Adv. Energy Mater.* **2012**, *2*, 400−409.
(26) Chen, S.; Walsh, A.; Gong, X. G.; Wei, S. H. Classification of Lattice Defects in The Kesterite Cu_2ZnSnS_4 and $Cu_2ZnSnSe_4$ Earth-Abundant Solar Cell Absorbers. *Adv. Mater.* **2013**, *25*, 1522−1539.
(27) Yin, X.; Tang, C.; Sun, L.; Shen, Z.; Gong, H. Study on Phase Formation Mechanism of Non- and Near-Stoichiometric $Cu_2ZnSn(S,Se)_4$ Film Prepared by Selenization of Cu−Sn−Zn−S Precursors. *Chem. Mater.* **2014**, *26*, 2005−2014.
(28) Zhou, H.; Song, T. B.; Hsu, W. C.; Luo, S.; Ye, S.; Duan, H. S.; Hsu, C. J.; Yang, W.; Yang, Y. Rational Defect Passivation of $Cu_2ZnSn(S,Se)_4$ Photovoltaics with Solution-Processed Cu_2ZnSnS_4:Na Nanocrystals. *J. Am. Chem. Soc.* **2013**, *135*, 15998−16001.
(29) Johnson, M.; Baryshev, S. V.; Thimsen, E.; Manno, M.; Zhang, X.; Veryovkin, I. V.; Leighton, C.; Aydil, E. S. Alkali-Metal-Enhanced Grain Growth in Cu_2ZnSnS_4 Thin Films. *Energy Environ. Sci.* **2014**, *7*, 1931−1938.
(30) Sutter-Fella, C. M.; Stückelberger, J. A.; Hagendorfer, H.; La Mattina, F.; Kranz, L.; Nishiwaki, S.; Uhl, A. R.; Romanyuk, Y. E.; Tiwari, A. N. Sodium Assisted Sintering of Chalcogenides and Its Application to Solution Processed $Cu_2ZnSn(S,Se)_4$ Thin Film Solar Cells. *Chem. Mater.* **2014**, *26*, 1420−1425.